for the case that the cloud consists of dark dust particles. If the particles are nitrogen ice crystals the flux limit would be roughly twice this value. As discussed earlier, the mass fraction of ice crystals could be about 5% and so the mass flux of vapor from west plume could be over 400 kg s^{-1}.

The heat of sublimation of solid N_2 is about 2.24×10^5 J kg^{-1}. Therefore, the power required to supply vapor at a rate of 400 kg s^{-1} is about 10^8 W. The solar power incident on Triton is about 1.5 W m^{-2}. Therefore, a solar collector area of about 10×10 km would be required to generate the required vapor if most (say ~2/3) of the solar energy were collected in the greenhouse to drive the process, which would be an exceedingly efficient case.

Assuming the numerous streaks seen on the subliming polar caps were produced earlier in the southern spring and summer by other geyser-like eruptions, we estimate the lifetime of such eruptions must be of the order of a year to several years. If it were much shorter, the probability of witnessing active eruptions would be too small; if it were much longer (comparable to Triton's seasons), more should have been seen.

Given a mass flux for nitrogen vapor as high as 400 kg s^{-1}, an eruption lifetime of 5×10^8 s would suggest a total erupted mass of 2×10^{11} kg. This is equivalent to 0.2 km^3 of nitrogen ice being sublimed during the eruption. For the collector area of 100 km^2 mentioned above, this would imply sublimation of 2 m of solid N_2 over the lifetime of the eruption. These estimates seem high and probably represent upper bounds, as the annual transport of N_2 from pole to pole is only of the order of a meter. Thus, the lower estimates of mass fluxes and lifetimes might be preferable.

REFERENCES AND NOTES

1. On Earth "geyser" denotes a reservoir of liquid water that intermittently erupts due to vapor formation during heating. In contrast, the word "fumarole" is typically restricted to a steam vapor vent where little or no liquid water is present in the reservoir. In this context, planetary geysers would correspond to initial conditions on the low-entropy side of temperature-entropy diagrams, whereas fumarole eruptions would correspond to eruptions from high-entropy conditions [see S. W. Kieffer, in *Satellites of Jupiter*, D. Morrison, Ed. (Univ. of Arizona Press, Tucson, 1982), p. 647]. In a strict thermodynamic sense, the phenomena that we discuss in this report may be fumarolic rather than geyser-like, but because possible models include both direct solid-to-vapor formation as well as liquid-to-vapor eruption, we choose to keep the more commonly used term "geyser." We note that planetary exploration is broadening our use of the terrestrial term "geyser" just as it has expanded our concept of "volcano."
2. B. A. Smith *et al.*, *Science* **246**, 1422 (1989).
3. D. P. Cruikshank, R. H. Brown, R. N. Clark, *Icarus* **58**, 293 (1984); D. P. Cruikshank, R. H. Brown, L. P. Giver, A. T. Tokunaga, *Science* **245**, 283 (1989).
4. R. H. Brown *et al.*, *Science* **250**, 431 (1990); R. L. Kirk *et al.*, *ibid.*, p. 424.
5. E. C. Stone and E. D. Miner, *ibid.* **246**, 1417 (1989); B. Conrath *et al.*, *ibid.*, p. 1454; G. L. Tyler *et al.*, *ibid.*, p. 1466.
6. W. R. Thompson, B. Murray, B. N. Khare, C. Sagan, *J. Geophys. Res.* **92**, 14933 (1987); L. J. Lanzerotti and W. L. Brown, in *Proceedings of the NATO Advanced Research Workshop on Ices in the Solar System* (Plenum, New York, 1984); G. Strazzulla, L. Calcano, G. Foti, *Mon. Not. R. Astron. Soc.* **204**, 59 (1983).
7. R. A. Jacobson, *Astron. Astrophys.* **231**, 241 (1990).
8. A. W. Harris, in *Uranus and Neptune*, J. Bergstralh, Ed. (NASA, Washington, DC, 1984); D. P. Cruikshank and R. H. Brown, in *Satellites*, J. A. Burns and M. S. Matthews, Eds. (Univ. of Arizona Press, Tucson, 1986), p. 836.
9. C. Sagan and C. Chyba, *Nature* **346**, 546 (1990).
10. C. J. Hansen *et al.*, *Science* **250**, 421 (1990).
11. R. V. Yelle *et al.*, *Icarus*, in press.
12. A. P. Ingersoll, *Nature* **344**, 315 (1990).
13. Entropies and enthalpies obtained from integration of heat capacity data in W. F. Giauque and J. O. Clayton, *J. Am. Chem. Soc.* **55**, 4875 (1933).
14. J. S. Turner, *J. Fluid Mech.* **26**, 779 (1966).

9 August 1990; accepted 27 September 1990

Color and Chemistry on Triton

W. Reid Thompson and Carl Sagan

The surface of Triton is very bright but shows subtle yellow to peach hues which probably arise from the production of colored organic compounds from $CH_4 + N_2$ and other simple species. In order to investigate possible relationships between chemical processes and the observed surface distribution of chromophores, we classify the surface units according to color/albedo properties, estimate the rates of production of organic chromophores by the action of ultraviolet light and high-energy charged particles, and compare rates, spectral properties, and expected seasonal redistribution processes to suggest possible origins of the colors seen on Triton's surface.

Before the Voyager encounter, spectroscopic measurements and modeling demonstrated the presence of CH_4 (*1, 1a, 2*) and suggested the presence of N_2 (*1a, 3*) on the surface of Triton. The production of simple and complex organic compounds, some white and some possessing yellowish hues, from charged particle and uv processing of mixtures of CH_4 and N_2 in the atmosphere and CH_4, H_2O, and/or N_2 on the surface was expected (*4*). Some quantity of Titan-like haze was also expected, but indications that Triton was probably bright and cold (*2*) suggested that this haze would be thin and the surface would be partially visible provided that N_2 condensate clouds (*5*) were also sufficiently thin.

Voyager observations confirmed the presence of CH_4 and N_2 (*6*) and revealed a very cold surface temperature of about 38 K (*7*) and pressure of about 16 μbar (*8*). The predominantly N_2 atmosphere is in vapor pressure equilibrium with darker portions of the large southern hemisphere cap (SHC) (*9*), while CH_4 is undersaturated, with an atmospheric mole fraction $X_{CH_4} \simeq 10^{-5}$ at the surface (*10*). Triton's surface is uniformly very bright (normal reflectance r_n typically 0.6 to 1.0), but has subtle hues which we collectively describe as yellow to "peach" over most of its surface (*11*). Major color/albedo units are obvious to subjective inspection: the apparently permanent SHC extending from the pole to about 15°S has a surface with relatively dark mottled areas ("splotches"), streaks, and irregular broken areas suggestive of a fragmented surface layer, while a very bright and white transient frost margin extends to and at some longitudes across the equator; this frost overlies a geologically complex equatorial terrain which is darker and more strongly colored than the SHC (*12*).

In this report we use a cluster analysis technique to identify the major spectral units distinguishable in the highest resolution full-disk multiband images of Triton, assess the major chemical processes producing chromophores there, and examine possible relationships between the spectral properties, chemistry, and seasonal cycles.

For color/albedo classification, we use five narrow-angle images of Triton at a phase angle of 39° in the UV, VI, BL, GR, and OR filters which are photometrically calibrated, located on the image frame by limb-fitting, and reprojected to provide a consistent geometry for classification (*13*). The shading due to varying illumination geometry across the disk was removed by an empirical photometric function with parameters determined by least-squares fitting (Table 1). The "normal" albedo r_n is formally equal to A and does not explicitly include phase effects. Because of superior photometric quality and wide wavelength spacing, the quantities R_{UV}, R_{BL}, and R_{OR} computed by dividing the disk intensity point-by-point by the photometric function were used in a three-parameter cluster analysis type of spectral classification (*14*). True color (*15*) and

Laboratory for Planetary Studies, Cornell University, Ithaca, NY 14853.

enhanced color versions of the processed images (Fig. 1) visually represent the digital database.

Cluster analysis indicates at least 60 statistically distinguishable units. Many of these units represent subdivisions along albedo gradients in specific geographic regions, so it is convenient to group them into larger classes. We identify six major classes of surface material. Two to four of the individual units constituting each of these classes are described in Table 2. Their geographic locations and mean broadband spectra (*16*) are shown in Fig. 2. The regular progression of albedo in the bright, moderately colored polar cap units (class I) suggests that they differ mostly in the quantity of admixed chromophore or overlying bright frost (or both), and not much in chromophore spectral properties. The bodies of dark streaks have spectral properties in common with larger dark patches on the cap. The streaks probably arise from material ejected by geysers and entrained in the prevailing wind or transported by saltation of low-cohesion particles (*17*). Very bright, neutral-white material (class II) extending into the equatorial region is probably seasonal frost thick enough to hide the underlying reddish substrate (*18*). The darker units northward of the equator are more strongly colored (class III). The relatively light unit 10 in this class also includes the darkest splotches on the polar cap, while the most highly colored material has a spectrum most similar to, but less VI and UV absorbing than, the global mean color observed in 1977, which is much "redder" than that observed in 1989 (*19*). Units constituting class IV are very UV-bright and probably represent varying depths of optically thin frost over class III material. Some UV-bright patches associated with dark streaks also belong to class IV. Class V and VI material is mostly confined to longitudes around 90°E. This different type of SHC material is characterized by areas showing OR absorption (class V) and small spots showing strong UV absorption (class VI) but relatively flat spectra otherwise. Some of our classes correspond to major spectral units derived by McEwen using a different method and the VI, CL, and GR normal albedos (*20*). After assessing chemical processes we assess possible relationships between chemistry and unit spectral properties.

Five major kinds of chemical processing can be identified: (i) photochemistry of CH_4 in the atmosphere by short-wavelength uv ($\lambda < 150$ nm) (*21*); (ii) radiation chemistry of $N_2 + CH_4$ initiated by high-energy electrons in the atmosphere (*22*); (iii) a small fraction of short-wavelength uv and $E \gtrsim 1$ MeV e^- which penetrates to the surface; (iv) medium-wavelength uv (150 nm $< \lambda <$ 190 nm) which acts on C_2H_4 and C_2H_2 ices produced by process (i); and (v) cosmic rays penetrating many meters into the surface (*3*). The rates of surface coloration computed (*23, 24*) for processes (ii) to (v) are given in Table 3.

This overall assessment of chemical processes suggests that a more or less global dusting of chromophores is provided at a steady rate by the action of medium wavelength uv upon C_2H_4 and C_2H_2 ices, which

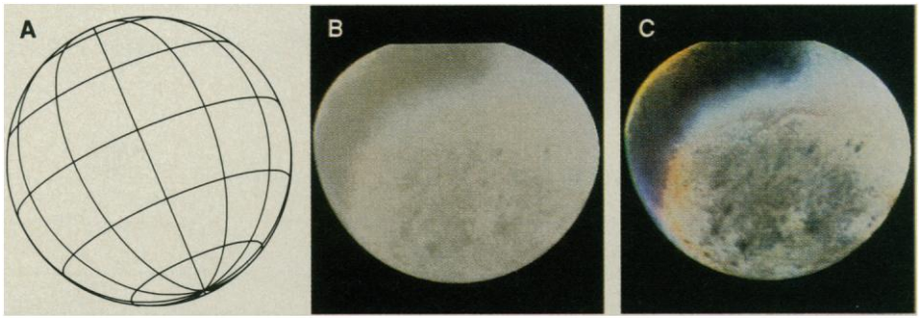

Fig. 1. Color images of Triton constructed from individual spectral bands reprojected to the same viewing geometry and resolution (15.7 km per pixel) used for color/albedo classification. (**A**) Latitude-longitude overlay grid with 30° spacing and the same aspect and size as the Triton images here and in Fig. 2. The intersection near disk center is 0° latitude and longitude; east longitude increases right from this point, and the south pole is just visible. (**B**) Natural color (red/green/blue) image (*15*); (**C**) OR/BL/UV image, visually representing the r_n databases used for classification, contrast enhanced.

Table 1. Least-squares photometric parameters for the Triton 39° phase images used in this study. The empirical function $I/F = [\mu_0 + (1 - \mu_0)\mu_c] \times \{A/[(\mu + \mu_o)/2]^k\}$ well represents the disk shading. The parameter A is formally the "normal albedo," I/F at a hypothetical $\mu = \mu_o = 1$; parameter μ_c accounts for limb brightening; and k is an adjustable exponent. Fits are limited to $\mu_0 > 0.2$. λ_{eff} is the solar flux–weighted effective wavelength of the indicated Voyager filters. (FDS refers to the flight data subsystem.)

FDS count	Filter	λ_{eff}	A	k	μ_c
11386.39	OR	0.589	0.8633	0.2209	0.0247
11387.03	GR	0.561	0.8640	0.1759	0.0055
11386.51	BL	0.481	0.8308	0.1817	0.0123
11387.09	CL	0.475	0.8207	0.0967	0.0301
11386.57	VI	0.414	0.8112	0.0989	0.0344
11387.15	UV	0.345	0.8119	0.0156	0.0604

Table 2. Mean spectral properties of selected clusters within each color/albedo class. See Fig. 2 for maps of unit locations on Triton's disk.

Class and description	Unit	Normal I/F (A term)				
		UV	VI	BL	GR	OR
I: Polar cap plus	6	0.881	0.874	0.889	0.926	0.918
equatorial band margin,	1	0.813	0.822	0.846	0.884	0.881
faint yellowish color,	3	0.789	0.792	0.810	0.847	0.846
7 includes some streaks	7	0.745	0.753	0.776	0.818	0.819
II: Thick frost at cap	11	0.974	0.937	0.918	0.938	0.925
edge very bright	13	1.021	0.982	0.943	0.970	0.926
and blue-white	15	0.992	0.920	0.896	0.902	0.875
	29	1.029	0.954	0.890	0.917	0.888
III: Equatorial region	10	0.665	0.678	0.706	0.770	0.758
orange units, darkest	16	0.528	0.605	0.645	0.733	0.716
cap blotches in 10,	22	0.483	0.587	0.638	0.711	0.690
22, 24 dark/reddish	24	0.504	0.580	0.605	0.706	0.682
IV: Frost leading edge,	26	0.936	0.858	0.824	0.849	0.835
very UV-bright,	19	0.889	0.831	0.806	0.832	0.825
21, 27 include some	21	0.850	0.782	0.760	0.801	0.801
streak areas	27	0.802	0.750	0.734	0.784	0.787
V: Polar cap bright area,	17	0.946	0.971	0.962	1.029	0.984
OR absorbing units	31	1.079	1.090	1.036	1.164	1.041
VI: Polar cap bright area,	42	0.983	1.101	1.059	—	1.071
UV absorbing units	52	0.969	1.088	1.055	—	1.050

are continuously produced from CH_4 by short wavelength uv primarily in the sunlit hemisphere (*25*). Direct chromophore production from CH_4 ice exposed at the surface occurs (aside from the thin veneer subject to uv) more slowly and only on very long time scales if overlain by $\gtrsim 1$ mm of N_2, which can easily be deposited in as little as 1 month in the equatorial region (*26*). In light of the chemical and spectral evidence, we offer the following nominal explanations.

Contrasts in the class I portions of the SHC are probably due to active redistribution of old chromophores since the thick N_2 frost deposits likely over such areas either permanently (*9*) or for most of a Triton year (*26*) are both poor in CH_4 and tend to protect any underlying CH_4 ice from direct radiation darkening. However, lag deposits may further darken if unprocessed C_2H_4 and C_2H_2 grains entrained with frost from the prior winter season constitute a portion of the involatile residue. Classes II and IV constitute transient, seasonal frost which, respectively, completely or incompletely covers the underlying material. Note that with the exception of thin frost associated with some streaks, frost of this type has not been deposited over the area of the SHC visible in these images.

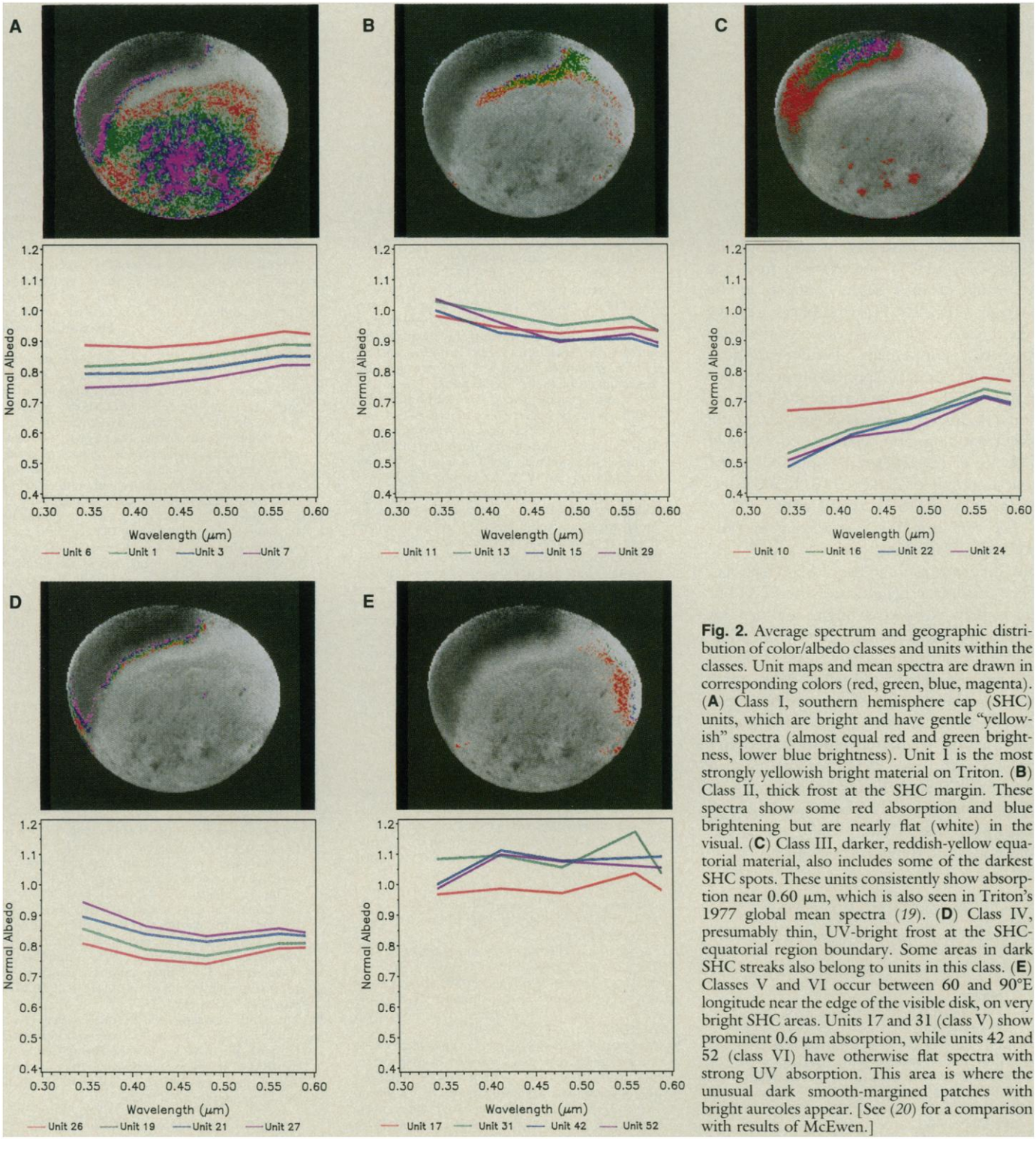

Fig. 2. Average spectrum and geographic distribution of color/albedo classes and units within the classes. Unit maps and mean spectra are drawn in corresponding colors (red, green, blue, magenta). (**A**) Class I, southern hemisphere cap (SHC) units, which are bright and have gentle "yellowish" spectra (almost equal red and green brightness, lower blue brightness). Unit 1 is the most strongly yellowish bright material on Triton. (**B**) Class II, thick frost at the SHC margin. These spectra show some red absorption and blue brightening but are nearly flat (white) in the visual. (**C**) Class III, darker, reddish-yellow equatorial material, also includes some of the darkest SHC spots. These units consistently show absorption near 0.60 μm, which is also seen in Triton's 1977 global mean spectra (*19*). (**D**) Class IV, presumably thin, UV-bright frost at the SHC-equatorial region boundary. Some areas in dark SHC streaks also belong to units in this class. (**E**) Classes V and VI occur between 60 and 90°E longitude near the edge of the visible disk, on very bright SHC areas. Units 17 and 31 (class V) show prominent 0.6 μm absorption, while units 42 and 52 (class VI) have otherwise flat spectra with strong UV absorption. This area is where the unusual dark smooth-margined patches with bright aureoles appear. [See (*20*) for a comparison with results of McEwen.]

Table 3. Energy sources for chemical processing of CH_4 or of simple hydrocarbons derived from atmospheric chemistry at Triton's surface, and characteristic time scales for significant coloration or darkening by the formation of organic heteropolymers (*3*). C_2H_4 and C_2H_2 produced by atmospheric chemistry are destroyed in less than one Triton year Y (as fast as they are produced), but require ~$6Y$ to build up a detectable quantity (~0.1 mg cm^{-2}) of new material.

Starting material	Energy scource	Penetration depth	Coloration/darkening time scale (Triton years)
C_2H_4 and C_2H_2	uv, $150 < \lambda < 190$ nm	1 μm	6
CH_4	Surface uv, $\lambda < 150$ nm	0.6 μm	6
Any hydrocarbon	Energetic electrons, $E \gtrsim 400$ keV	1 mm	700
Any hydrocarbon	Cosmic rays	1 m	2×10^6

Chromophores in the darker equatorial units should also be much older than seasonal time scales, yet the spectra of class III are systematically different from those of class I, trending toward concave downward as the albedo decreases; further, class I spectra typically have a near zero spectral gradient from GR to OR while all class III spectra have a decreasing gradient. Since most of Triton's surface must have spectroscopically visible CH_4 ice (*27*), and relatively frost-free ice would produce slight contrasts in the Voyager OR and CH_4-band filters (*28*), we take this evidence as suggestive of the presence of CH_4 or perhaps other hydrocarbons with similar near IR spectral properties (for example, C_2H_6) at the surface in all class III units. A different chromophore here could arise from long-term chemical processing of CH_4 ice at the surface, as opposed to the collection only of darkened C_2H_4 and C_2H_2 sediments in the SHC class I units.

The very bright UV-absorbing or OR-absorbing SHC units (classes V and VI) are very different from the class I SHC material. They may make up much of the SHC but are at high perspective angles and are not well sampled in these images. One plausible source for unusually colored SHC material is CH_4 frost which, unlike class III material, is fine-grained and subject to more rapid direct processing. Although limited resolution prevents secure identification, the dark features with irregular but smooth-rimmed margins and surrounding aureoles [figure 30 of Smith *et al.* (*12*)] occur at the longitudes where class V and VI units appear and may constitute some of these units.

REFERENCES AND NOTES

1. D. P. Cruikshank and J. Apt, *Icarus* **58**, 306 (1984).
1a. D. P. Cruikshank, R. H. Brown, A. T. Tokunaga, R. G. Smith, J. R. Piscitelli, *ibid.* **74**, 413 (1988).
2. W. R. Thompson, *Geophys. Res. Lett.* **16**, 969 (1989).
3. D. P. Cruikshank, R. H. Brown, R. N. Clark, *Icarus* **58**, 293 (1984).
4. M. L. Delitsky and W. R. Thompson, *ibid.* **70**, 354 (1987); W. R. Thompson *et al.*, *J. Geophys. Res.* **92**, 14933 (1987); J. R. Piscitelli, D. P. Cruikshank, J. F. Bell, *Icarus* **76**, 118 (1988); W. R. Thompson, S. K. Singh, B. N. Khare, C. Sagan, *Geophys. Res. Lett.* **16**, 981 (1989).
5. C. P. McKay, J. B. Pollack, A. P. Zent, D. P. Cruikshank, R. Courtin, *Geophys. Res. Lett.* **16**, 973 (1989).
6. A. L. Broadfoot *et al.*, *Science* **246**, 1459 (1989).
7. B. Conrath *et al.*, *ibid.*, p. 1454.
8. G. L. Tyler *et al.*, *ibid.*, p. 1466.
9. A. S. McEwen, *Geophys. Res. Lett.* 17, 1733.
10. See Broadfoot *et al.* (*6*). The mole fraction if both gases were saturated is ~1.5×10^{-4} at 38 K [G. N. Brown, Jr., and W. T. Ziegler, *Adv. Cryog. Eng.* **25**, 662 (1980)].
11. See Smith *et al.* (*12*). Most of Triton's surface has a subtle, nearly linear slope from the OR filter (0.59 μm) to UV (0.35 μm); its color can be determined quantitatively [see Fig. 1 and (*15*)].
12. B. A. Smith *et al.*, *Science* **246**, 1422 (1989).
13. These images were obtained from a distance of 530,000 to 502,000 km about 2 hours before Neptune's closest approach. Other images were reprojected to the perspective of the VI image. For building databases of manageable size for classification, images were sampled at 15.7 km per pixel resolution at the sub-spacecraft point.
14. The cluster analysis method is a hybrid method in which the entire collection of objects is first condensed to about 1000 preliminary clusters by a least-squares method, then hierarchically merged, tracking three statistical measures to determine the number of clusters. See W. R. Thompson, *Int. J. Supercomput. Appl.* **4**, 48 (1990), and references therein.
15. Constructing "true color" here consists of interpolating images taken through the Voyager filters (see Table 1) to the mean wavelengths of the human blue, green, and red visual response (respectively, ~0.445, 0.555, and 0.600 μm). The formulas used were $Red = 0.102 \times (R_{OR} - R_{BL}) + R_{OR}$; $Green = 0.685 \times (R_{OR} - R_{BL}) + R_{BL}$; $Blue = 0.265 \times (R_{UV} - R_{BL}) + R_{BL}$. The resulting photographic product is then verified by computing chromaticities and comparing the product with color standards. In coordinates (x, y, Y) [see F. W. Billmeyer, Jr., and M. Saltzman, *Principles of Color Technology* (Wiley, New York, ed. 2, 1981)], the disk-average chromaticity is (0.337, 0.338, 0.82), close to Munsell color 9/2 7.5YR. The steeper spectrum observed in 1977 (*19*) has chromaticity (0.347, 0.356, 0.78), close to Munsell color 9/3 2.5Y.
16. Substantial parts of the disk are truncated on the VI and GR images of this sequence. For computation of mean spectra, only pixels which appear on all five images (or all except GR for class six) are used.
17. See Smith *et al.* (*12*); L. A. Soderblom *et al.*, *Science* **250**, 410 (1990); C. Sagan and C. Chyba, *Nature* **346**, 546 (1990).
18. Figure 29 in Smith *et al.* (*12*) shows that this frost overlies parts of the equatorial region beyond the SHC margins. McEwen (*9*) also identifies this unit with thick frost.
19. See spectra in Thompson (*2*) and Smith *et al.* (*12*). The disk-average spectrum of Triton changed remarkably between 1977 and 1989, yet the visual magnitude appeared to stay constant [N. L. Lark, H. B. Hammel, D. P. Cruikshank, D. J. Tholen, M. A. Rigler, *Icarus* **79**, 15 (1989)].
20. McEwen (*9*) identifies six spectral units in an assessment of global color/albedo properties using a manual classification based on inspection of multispectral mosaics and a 2D histogram of the CL albedo and GR/VI ratio. These units have approximate equivalents in our classes or units. M1 (McEwen unit 1) is dark reddish equatorial material and corresponds to C3 (our class III); M5 is the major portion of the SHC material and corresponds to the lighter units 6 and 1 in C1; M2 is darker SHC material and corresponds to our C1 unit 7 and the SHC portion of C3 unit 10; M6 is the bright, blue-white SHC margin and corresponds to C2; M4 is thin frost over the equatorial region and corresponds to C4; M3 is the redder bright material in the SHC and corresponds to part of C1 unit 1. There is no equivalent to our bright, anomalously colored C5 and C6. McEwen's units are more areally contiguous, while our results are not constrained in this way, and show for example that redder SHC material (M3, C1 unit 1) is scattered in fragmentary patches across the SHC, and that bright spots at the origin of SHC streaks are spectrally the same as thin frost at the SHC margin (C4 units 21 and 27). The good S/N and minimal smear of the images we use ensure that this fine structure is real.
21. D. F. Strobel *et al.*, *Geophys. Res. Lett.* 17, 1729 (1990).
22. W. R. Thompson *et al.*, in (*4*); see also W. R. Thompson, T. J. Henry, J. M. Schwartz, B. N. Khare, C. Sagan, *Icarus*, in press.
23. We use a representative electron differential energy spectrum at Triton's orbit and cosmic ray and solar uv fluxes with methods applied previously [C. Sagan and W. R. Thompson, *Icarus* **59**, 133 (1984); M. L. Delitsky and W. R. Thompson, in (*4*)] to compute (ii) to (v) for Triton's current atmospheric conditions. C_2H_4, C_2H_2, and C_2H_6 are produced (*21*) by process (i) at respective rates of 7, 5, and 4 μg cm^{-2} per Triton year Y (165 Earth years). However, process (iv) converts C_2H_4 and C_2H_2 to more complex products, at least some of which are colored at a rate of 15 μg cm^{-2} Y^{-1}. Process (ii) supplies NH_3 and C_2H_2 at rates around 1.6 μg cm^{-2} Y^{-1}, HCN at 0.5 μg cm^{-2} Y^{-1}, and other nitriles at lower rates (*24*). About 20% of Ly-α radiation penetrates to the surface, but can act on only a very thin veneer of exposed hydrocarbons. Magnetospheric electrons and cosmic rays penetrate deeper but produce chromophores more slowly. The atmospheric structure used in the computations is from Broadfoot *et al.* (*6*). The Voyager 2 electron spectrum at 14.2 Neptune radii (outbound) was supplied by L. Lanzerotti and S. M. Krimigis.
24. The results of Thompson *et al.* (*22*) were generated for a pre-Voyager estimate of 0.3 erg cm^{-2} s^{-1} of energetic electrons and an experimental gas mixture of 10^{-3} CH_4 in N_2. Integration of the measured electron spectrum gives a nearly identical energy input 0.29 erg cm^{-2} s^{-1}, but a downward correction of a factor of at least 10 in production rates is estimated because of the lower $X_{CH_4} \simeq 2 \times 10^{-6}$, appropriate to 40 km altitude in Triton's atmosphere [extrapolated from Broadfoot *et al.* (*6*)]. Thus results of Thompson *et al.* (*22*) were reduced by a factor of 10 to derive the numbers given.
25. See (*21*). At Neptune's distance from the sun, interstellar Ly-α contributes a substantial fraction of the total flux, so some photochemistry also occurs in the dark hemisphere.
26. J. A. Stansberry, J. I. Lunine, C. C. Porco, A. S. McEwen, *Geophys. Res. Lett.* 17, 1773 (1990); J. R. Spencer, *ibid.*, p. 1769.
27. J. R. Spencer, M. W. Buie, and G. L. Bjoraker (*Icarus*, in press) estimate that less than 35% of the projected area of the surface is covered by material which is bright at $\lambda = 3.2$ μm, implying 65% areal coverage of ice with at least enough CH_4 to be dark at this wavelength.
28. See (*2*). Clean CH_4 ice would have about a 3% contrast in the narrow-angle OR filter and wide-angle CH_4 − U filter, about 5% contrast in the wide-angle OR filter, and ≳20% contrast in the wide-angle CH_4 − J filter. Images at about 10 km per pixel resolution and 65° phase are available in the broadband filters plus CH_4 − U.

29. This work was supported by the Voyager Project and the NASA Planetary Geology and Geophysics program. We thank the Cornell Theory Center and the IBM Corp. for providing computing resources, and Voyager imaging team leader B. Smith for providing supplemental funds.

9 August 1990; accepted 24 September 1990